# Homology Modeling and Docking Analysis of the Interaction between Polyphenols and Mammalian 20S Proteasomes

Matteo Mozzicafreddo,* Massimiliano Cuccioloni, Valentina Cecarini, Anna Maria Eleuteri, and Mauro Angeletti

MCAB Department, University of Camerino, 62032 Camerino (MC), Italy

Received July 14, 2008

Molecular docking of small ligands to biologically active macromolecules has become a valuable strategy to predict the stability of complexes between potential partners and their binding modes. In this perspective, we applied this computational procedure to rationalize the reported role of polyphenols as inhibitors of the mammalian 20S proteasomes. In particular, polyphenols were shown to modulate each proteasomal activity at different extents both in the constitutive and the inducible enzyme. We performed a flexible molecular docking analysis between a set of polyphenols previously demonstrated to have the highest binding affinity and both the constitutive (from deposited PDB structures) and homology modeled active subunits of the IFN-$\gamma$ inducible proteasome, to provide insight into the possible mechanism of interaction. Among the tested polyphenols, (-)-epigallocatechin-3-gallate showed the highest affinity for the proteasome subunits, both in terms of intermolecular energy and predicted equilibrium constants, in particular for $\beta$5 and $\beta$5i subunits ($E_{Total}$=−66 kcal/mol, $K_i$=81.3 $\mu$M and $E_{Total}$=−83.9 kcal/mol, $K_i$=0.29 $\mu$M, respectively), known to be related to the chymotrypsin-like and BrAAP activities. Collectively, polyphenols showed a higher affinity for the inducible subunits, in agreement with previous *in vitro* studies. Additionally, different contributions to the interaction energy (van der Waals, electrostatic, H-bond) of proteasome-polyphenols complexes were dissected.

## INTRODUCTION

Several biological processes, e.g. signal transductions, physiological regulation, gene transcription, and enzymatic reactions, are based on ligand-binding interactions. These interactions involve both macromolecular complexes (e.g., protein−protein and protein−DNA)[1−5] and complexes where macromolecules combine with small molecules.[6−11]

Consequently, a thorough understanding of ligand-binding interactions between small molecules and proteins is crucial in the development of a strategy for a rational drug design, since it is less cost- and time-consuming than the traditional screening protocols for drug discovery, and then it may help develop more selective therapeutic agents, reducing the undesiderable side effects.[12]

High-resolution structural data are now easily available for many important ligand−protein complexes thanks to technical improvement in X-ray crystallography, multidimensional NMR spectroscopy, and other structural characterization methods. Sometimes it is even possible to generate approximate three-dimensional models for receptor proteins through computational procedures such as homology model building.[13,14] Moreover, it is feasible to obtain detailed computational analyses and design projects for ligand−receptor complexes thanks to advanced molecular modeling tools and several available computing resources.[15−17]

Herein we report on the application of these computational approaches to the analysis of the interaction between some natural occurring polyphenols and mammalian 20S proteasome.

The mammalian proteasome is a multisubunit and multicatalytic protease complex involved in various protein degradation processes.[18−20] It is characterized by a cylinder-shaped quaternary structure consisting of four heptameric rings, $\alpha_7\beta_7\beta_7\alpha_7$, with 7 distinct α-type and 7 distinct $\beta$-type subunits, and with C2 symmetry similar to those of the yeast.[21] In particular, three active subunits, $\beta$1, $\beta$2, and $\beta$5, are responsible for the three major proteolytic activities, the peptidylglutamil-hydrolyzing (PGPH), trypsin-like (T-L), and chymotrypsin-like (ChT-L) activities, respectively.[20,22−24] After the induction by interferon-$\gamma$ (IFN-$\gamma$), leading to the formation of the immunoproteasome, which is involved in the generation of the antigenic peptides,[25−28] three additional $\beta$ subunits, $\beta$1i, $\beta$2i, and $\beta$5i, replace the constitutive active subunit $\beta$1, $\beta$2, and $\beta$5, respectively.

All these proteolytic activities depend on the N-terminal threonine ($Thr^1$) residue hydroxyl group, which is responsible for catalyzing the cleavage of peptides through nucleophilic attack.[20]

Among small molecules inhibitors of proteasomal activity, polyphenols, in particular flavonoids, are a group of naturally occurring compounds ubiquitous in fruits and vegetables with antioxidant,[29] antiallergic,[30] anti-inflammatory,[31,32] cytoprotective,[33] and anticarcinogenic activities.[34,35]

These activities can be attributable to the ability of polyphenolic compounds to act either as mere reducing agents and free radical scavengers[36−38] or as specific ligands/effectors toward important metabolic enzymes like several

* Corresponding author phone and fax: +39 737403247; e-mail: matteo.mozzicafreddo@unicam.it. Corresponding author address: via Gentile III da Varano, 62032 Camerino (MC), Italy.

10.1021/ci800235m CCC: $40.75 
Published on Web 01/28/2009

serine proteases,[7,8,39−42] dihydrofolate reductase,[43−45] and other regulatory proteins.[46]

Additionally, green tea polyphenols (GTPs) containing ester bond(s), such as (-)-epigallocatechin-3-gallate, and other polyphenols, like quercetin, luteolin, gallic acid, etc., were reported to inhibit proteasomal activity both *in vitro* and *in vivo*.[47,48]

On such a basis, our study was intended to define the mechanisms underlying the inhibition of proteasomal activities by this class of small molecules.

## METHODS

**Homology Modeling Analysis of the Inducible Catalytic β Subunits.** Homology modeling is a computational procedure that allows for the building of a protein model (for unknown crystallographic structure) using several structural templates (proteins of known structure).[14] In particular, we used Swiss-Model[49] to derive the three-dimensional structure of immunoproteasome subunits ($\beta$1i, $\beta$2i, and $\beta$5i) from their amino acid sequences (query sequence).

The project file was built using Swiss-PdbViewer (version 3.7) and default parameter settings (BLAST search P value <0.00001; global degree of sequence identity SIM > 25%). The knowledge-based homology model was constructed on the Web server using the ProModII program,[50] and the model thus built was energy minimized using the Gromos96 force field.[51] The model coordinates were returned in PDB format.[14]

1iruH, with a sequence identity of 62%,[21] 1g0uN,[52] 1g652,[53] 2f162,[54] and 2fak2[55] were selected as structure templates for the $\beta$1i sequence; 1iruI, with a sequence identity of 58%,[21] 1g0uV,[52] 1jd2H,[56] and 1z7qW[57] were selected for the $\beta$2i sequence; 1iruL, with a sequence identity of 70%,[21] 1g0uY,[52] 2f16Y,[54] and 2fakK[55] were selected for the $\beta$5i sequence. All query sequences (regarding bovine and yeast proteasomes) were obtained from UniProt Knowledgebase (http://beta.uniprot.org/).

**Molecular Docking of the Complex between Proteasome Subunits and Polyphenols.** Molecular docking was performed on a Linux Red Hat Pentium4-based platform using the Docking and the Discover module of InsightII software (release 2005, Accelrys Ltd., Cambridge, U.K.). Mammalian (bovine liver) proteasome constitutive $\beta$ chains X-ray crystal structure (1iru[21]) were obtained from the Protein Data Bank.[58] Thirty rotamers of each polyphenol molecule (Figure 1) were generated and optimized by the Discover module and were positioned in proximity to the active site. The starting position of the ligand at a distance of 10 Å from the binding site (within a 15 Å radius sphere around Thr[1]) was randomly (Box-Muller) chosen each time. Hydrogen atoms were added to proteasome subunits, and resulting structures were minimized (using the consistent valence force field and conjugate gradients algorithm to a rms derivative of 0.001 kcal/mol) and checked using ProCheck v3.4.[59] The docking procedure was carried out constraining the enzyme being blocked and rigid, and the ligand being flexible, up to the minimum intermolecular energy condition and a rms derivative of 0.001 kcal/mol. The most stable composite $\beta$ subunit-polyphenol model (the highest LUDI score) was geometry minimized within the binding site (allowing the protein, within a 15 Å radius sphere around Thr[1], and the ligand to be flexible) by the means of the Discover module, fixing the rest of the protein. Other parameters were set as default (Charges: on; Cross: off; Morse: off; Dielectric: 1.00). All the results are obtained in terms of intermolecular energy ($E_{Total} = E_{Elect} + E_{VdW}$) and predicted inhibition constants $K_i$ derived from LUDI Score, using a standard equation ($LUDI\ Score = -100 \times log_{10}\ K_i$) and Energy Estimate 3 as scoring function.[15]

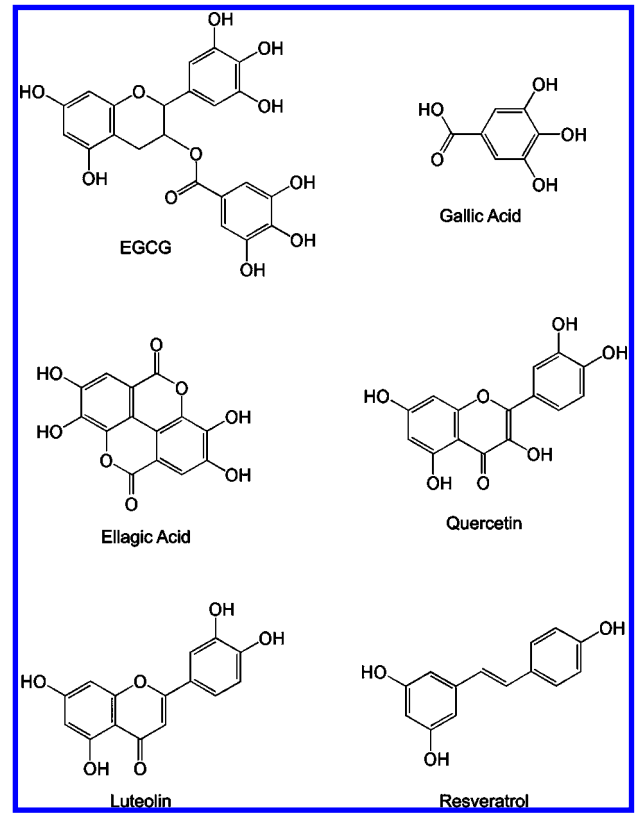


**Figure 1.** Molecular structures of the polyphenols used in the present study.

Clioquinol was used as a negative control, since it did not exhibit any relevant effect on proteasomal activity.[60]

The output from InsightII, all modeling studies, and images were rendered with PyMOL (2006, DeLano Scientific LLC, San Carlos, CA). PyMOL was also used to calculate the distances of hydrogen bonds as measured between the hydrogen and its assumed binding partner.

**Evaluation of the Differences in α-Carbon Position between Constitutive and Immunoproteasomes.** The differences in terms of distances between the corresponding α-carbons of the 20S proteasome crystallographic structure (1iru[21]) and the homology modeled immunoproteasome were calculated with a program developed under Python 2.5. This program routinely reads the x, y, z coordinates of each α-carbon and calculates the resulting rms distances according to a classic geometric relationship.[61] The resulting values were normalized to a suitable range and finally visualized on the output PDB file using a temperature-color scale by PyMOL software.

**Effect of Polyphenols on the 20S Proteasome Functionality.** The effects of quercetin and resveratrol on the $\beta$1 subunit activity and the effects of luteolin and ellagic acid on the $\beta$2i subunit activity were investigated through *in vitro* assays using fluorogenic peptides substrates (Z-Leu-Leu-Glu-AMC and Z-Leu-Ser-Thr-Arg-AMC, respectively).[62,63] Polyphe-

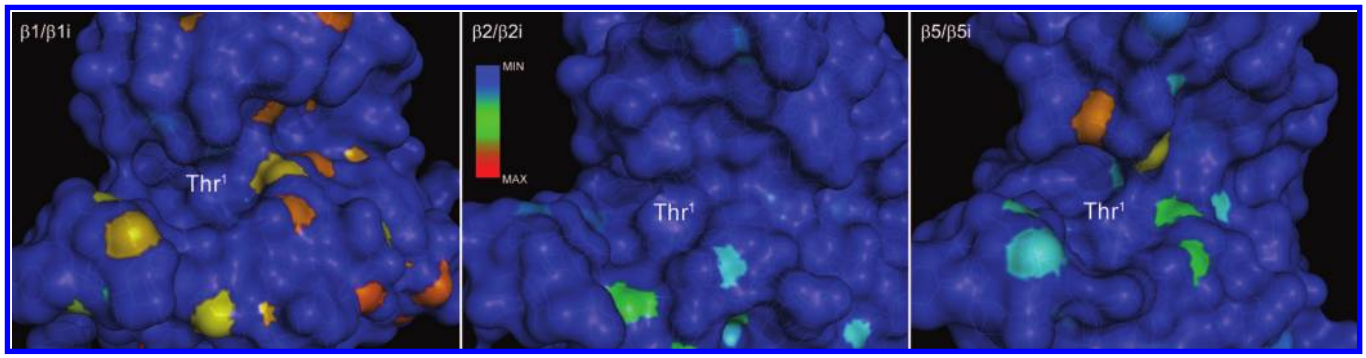


**Figure 2.** Visualization of different position of corresponding α-carbons in immuno- and constitutive $\beta$ subunits. The distances are expressed on a colorimetric scale ranging from blue (minimal difference) to red (maximal difference).

nols and proteasome substrates were purchased from Sigma-Aldrich S.r.L., Italy. Isolation and purification of the 20S proteasome from bovine brain was performed as previously reported.[64]

A mixture containing the polyphenol at different concentrations, 5 $\mu$g of the isolated constitutive 20S proteasomes, the appropriate substrate, and 50 mM Tris-HCl pH 8.0 up to a final volume of 500 $\mu$L was incubated at 37 °C for 60 min. Measurements of the hydrolyzed 7-amino-4-methylcoumarin (AMC) were performed (AMC: $\lambda_{exc}$=365 nm, $\lambda_{em}$=449 nm) on a spectrofluorimeter Shimadzu RF5301. The $K_i$ values were calculated from the residual activities, as previously described.[7,8]

## RESULTS AND DISCUSSION

Several studies on flavonoids binding modes to proteasome $\beta$5 subunit are currently available,[65,66] globally revealing the presence of a flavonoid replacing group susceptible to nucleophilic attack, a binding pose that places that group near the hydroxyl group of the protease N-terminal threonine, and a binding pose that locates the A-C ring system within or near the S1 pocket.

On such a basis, this investigation was intended to expand our knowledge of the possible interaction between other polyphenols and all catalytic proteasome subunits, for the first time extending the study to the immunocounterparts.

A homology model of immunoproteasome $\beta$-subunits was assembled with Swiss-Model using different $\beta$-subunit-like structural templates (see the Methods section). The quality and reliability of the model was assessed through a theoretical evaluation of the model. Stereochemical and energetic properties and the packing environment of its residues were comparable to those of the template subunits, as confirmed by Ramachandran plot analysis[67] (data not shown). Moreover, the results obtained with ProCheck v3.4[59] (data not shown) showed that backbone and side-chain conformations, bond lengths, angles, and residue contacts of the immunoproteasome $\beta$-subunits models are well within the criteria that have been established for reliable structures and are of almost as good quality as those of the reference subunits.

The comparison (of α-carbon positions, without side-chains contributions) between immuno- and constitutive $\beta$ subunits revealed that the α-carbon positions were highly conserved, particularly in $\beta$2 subunits (between immuno- and constitutive counterparts), both in terms of structure and function of the active site neighbors (Figure 2). In fact, the high structural similarity of $\beta$2 and $\beta$2i subunits produces a comparable behavior toward the studied polyphenols. Concerning specificity, the polyphenols studied can be put on the same affinity scale for both the $\beta$2 subunits. Conversely, although the $\beta$1 subunits present several major differences in α-carbons positions, the $\beta$5 subunits showed some crucial differences in the neighborhood of Thr[1] around the S1 pocket (Figure 2), likely to cause the subtle discrepancies in terms of inhibitory efficacy. In particular, luteolin and quercetin are differently recognized by $\beta$5 and $\beta$5i subunits (see Figure 3).

Then, polyphenols were independently docked onto each single catalytic $\beta$ subunit of both constitutive and inducible proteasome, and the results obtained after geometry minimization were expressed in terms of LUDI Score, predicted inhibition constants, intermolecular energies, and their components (van der Waals and electrostatic energies), as summarized in Table 1.

Collectively, our results are consistent with the presence of a specific binding site for monomeric polyphenols compounds on $\beta$ subunits: in fact, all polyphenols bind to the same catalytic sites (Figures 4−6), supporting their role as competitive inhibitors of single proteasomal activities.

The complexes between EGCG and $\beta$5 subunit, from both constitutive and inducible proteasome, related to the chymotrypsin-like and BrAAP activities, reported the highest stability in term of intermolecular energies, and predicted inhibition constants.

The inhibition of trypsin-like activity by EGCG here reported was in contrast to previous works[68] reporting EGCG inability to inhibit this proteasomal activity. Nevertheless, this discrepancy was only apparent, since those measurements were carried out in cell extracts rather than in an isolated enzymatic system; more importantly, EGCG levels used in that assay were too low to allow the evaluation of the inhibitory effect of a ligand having a $K_i$=180 $\mu$M (Table 1).

The EGCG/$\beta$1 and EGCG/$\beta$1i complexes were characterized by a favorable insertion of the A-C ring system of the polyphenol within the S1 hydrophobic pocket of the subunit (Figure 4), consistent with previous evidence on another predicted model.[66] Conversely, the other subunits accommodated EGCG in a different manner: in fact, the A-C ring insertion of EGCG within the catalytic site did not result in a most stable complex. In these cases, the most stable composite models for EGCG binding to $\beta$5 and $\beta$5i proteasome subunits were characterized by a limited insertion of the ligand within the S1 pocket (Figure 6), instead evidencing

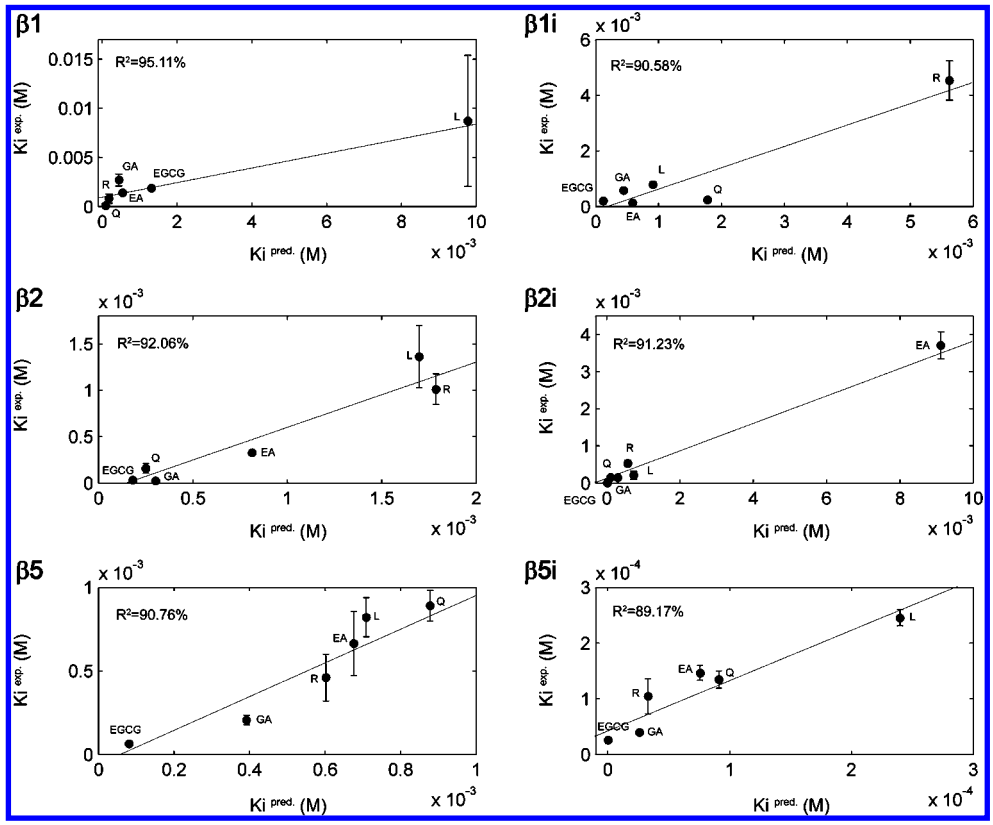


**Figure 3.** Linear dependence of previously reported experimental dissociation equilibrium constants[48] from predicted dissociation equilibrium constants of the complexes between polyphenols and catalytic proteasome subunits.

**Table 1.** Predicted Inhibition Constants, LUDI Scores, Total Intermolecular Energies (kcal/mol) (with van der Waals and Electrostatic Components), and Theoretical Number of H-Bond Formed into the Complexes between Polyphenols and Catalytic Proteasome Subunits

| | β1 | | | | | | β1i | | | | | |
|---|---|---|---|---|---|---|---|---|---|---|---|---|
| | $K_i$ (M) | LUDI | $E_{Total}$ | $E_{VdW}$ | $E_{Elect}$ | H-bond | $K_i$ (M) | LUDI | $E_{Total}$ | $E_{VdW}$ | $E_{Elect}$ | H-bond |
| EGCG | $1{,}32\cdot10^{-3}$ | 288 | −52,0715 | −41,9439 | −10,1276 | 4 | $1{,}20\cdot10^{-4}$ | 392 | −63,1542 | −46,0423 | −17,112 | 4 |
| EA | $5{,}49\cdot10^{-4}$ | 326 | −52,4162 | −37,4114 | −15,0048 | 7 | $5{,}89\cdot10^{-4}$ | 323 | −54,6642 | −42,1933 | −12,4709 | 2 |
| GA | $4{,}47\cdot10^{-4}$ | 335 | −35,5707 | −18,5058 | −17,0649 | 4 | $4{,}45\cdot10^{-4}$ | 335 | −40,3121 | −23,1025 | −17,2096 | 3 |
| Q | $9{,}12\cdot10^{-5}$ | 404 | −51,1657 | −34,3995 | −16,7663 | 7 | $1{,}78\cdot10^{-3}$ | 275 | −54,676 | −47,1105 | −7,56552 | 1 |
| L | $9{,}77\cdot10^{-3}$ | 201 | −49,6609 | −35,9398 | −13,7211 | 5 | $9{,}12\cdot10^{-4}$ | 304 | −52,5912 | −43,7301 | −8,86107 | 3 |
| R | $1{,}78\cdot10^{-4}$ | 375 | −45,6542 | −35,5134 | −10,1408 | 1 | $5{,}62\cdot10^{-3}$ | 225 | −58,6435 | −39,8454 | −18,7982 | 4 |
| | β2 | | | | | | β2i | | | | | |
| | $K_i$ (M) | LUDI | $E_{Total}$ | $E_{VdW}$ | $E_{Elect}$ | H-bond | $K_i$ (M) | LUDI | $E_{Total}$ | $E_{VdW}$ | $E_{Elect}$ | H-bond |
| EGCG | $1{,}82\cdot10^{-4}$ | 374 | −56,3675 | −36,9596 | −19,4079 | 2 | $2{,}24\cdot10^{-5}$ | 465 | −75,1991 | −49,2483 | −25,9508 | 8 |
| EA | $8{,}13\cdot10^{-4}$ | 309 | −45,8265 | −34,5107 | −11,3158 | 6 | $9{,}12\cdot10^{-3}$ | 204 | −44,917 | −28,0828 | −16,8342 | 2 |
| GA | $3{,}02\cdot10^{-4}$ | 352 | −34,7064 | −20,9078 | −13,7986 | 5 | $3{,}02\cdot10^{-4}$ | 352 | −32,6288 | −19,6866 | −12,9422 | 3 |
| Q | $2{,}51\cdot10^{-4}$ | 360 | −44,1811 | −31,9084 | −12,2727 | 4 | $1{,}09\cdot10^{-4}$ | 396 | −49,4916 | −34,9929 | −14,4386 | 4 |
| L | $1{,}69\cdot10^{-3}$ | 277 | −44,7561 | −34,1891 | −10,567 | 3 | $7{,}41\cdot10^{-4}$ | 313 | −45,8149 | −34,5092 | −11,3057 | 2 |
| R | $1{,}79\cdot10^{-3}$ | 275 | −49,6499 | −33,6648 | −15,9851 | 2 | $5{,}75\cdot10^{-4}$ | 324 | −50,7575 | −39,0659 | −11,6916 | 4 |
| | β5 | | | | | | β5i | | | | | |
| | $K_i$ (M) | LUDI | $E_{Total}$ | $E_{VdW}$ | $E_{Elect}$ | H-bond | $K_i$ (M) | LUDI | $E_{Total}$ | $E_{VdW}$ | $E_{Elect}$ | H-bond |
| EGCG | $8{,}13\cdot10^{-5}$ | 409 | −66,005 | −48,1308 | −17,8742 | 4 | $2{,}95\cdot10^{-7}$ | 653 | −83,932 | −58,1501 | −25,7819 | 5 |
| EA | $6{,}76\cdot10^{-4}$ | 317 | −49,938 | −29,8695 | −20,0685 | 5 | $7{,}59\cdot10^{-5}$ | 412 | −55,9281 | −42,1834 | −13,7448 | 4 |
| GA | $3{,}92\cdot10^{-4}$ | 341 | −39,414 | −25,5142 | −13,8998 | 6 | $2{,}61\cdot10^{-5}$ | 458 | −38,9337 | −27,6681 | −11,2656 | 5 |
| Q | $8{,}78\cdot10^{-4}$ | 306 | −54,9124 | −35,522 | −19,3903 | 3 | $9{,}12\cdot10^{-5}$ | 404 | −53,2853 | −38,5064 | −14,7789 | 3 |
| L | $7{,}09\cdot10^{-4}$ | 315 | −51,5519 | −36,5174 | −15,0346 | 3 | $2{,}39\cdot10^{-4}$ | 362 | −46,3926 | −38,5879 | −7,80474 | 3 |
| R | $6{,}02\cdot10^{-4}$ | 322 | −49,3278 | −38,9001 | −10,4278 | 3 | $3{,}31\cdot10^{-5}$ | 448 | −48,2756 | −33,3451 | −14,9305 | 2 |

a partial occlusion of the site as a result of mainly hydrophobic interactions with the S1 neighbors.

Globally, such an orientation/conformation of the EGCG in the proximity to the N-terminal Thr[1] of catalytic subunits was subject to nucleophilic attack at the galloyl moiety (in agreement with other authors[66]).

The other flavonoids (luteolin and quercetin, in particular) reported different and singular behavior, arbitrarily accommodating the A-C ring system within or outside the S1 hydrophobic pocket, despite the catalytic site geometry. This higher conformational freedom may be an effect of the smaller size of these polyphenols in comparison with EGCG,

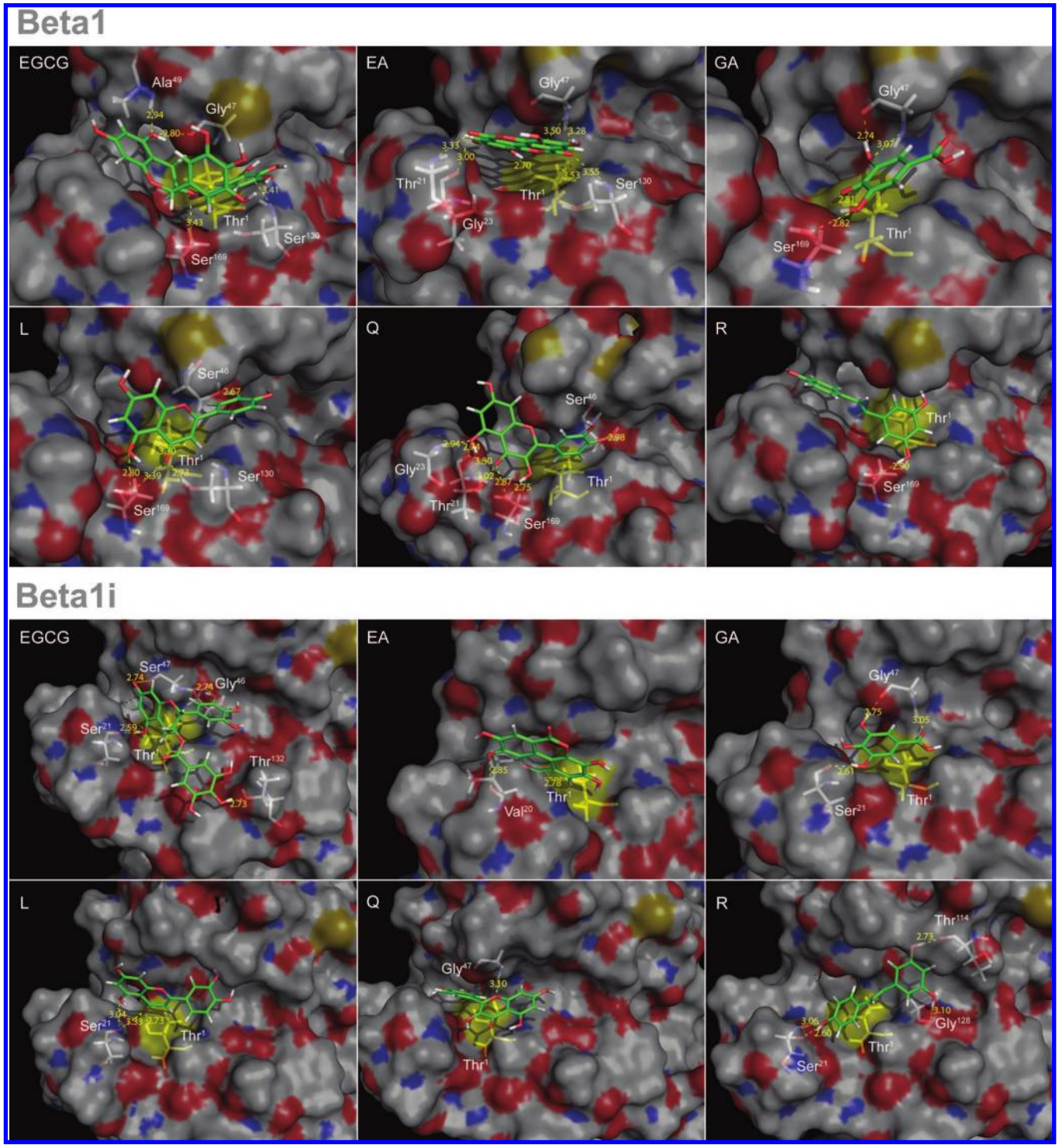


**Figure 4.** Three-dimensional representation of molecular docking of all polyphenols onto $\beta$1 and $\beta$1i subunits. The threonine catalytic residue (in bright yellow) and all amino acids involved in the formation of H-bonds with the polyphenols are highlighted. Moreover, oxygen, sulfur, nitrogen, and hydrogen atoms are colored in red, orange, blue, and white, respectively. All molecular complexes were rendered by PyMOL software.

this latter being more sterically constricted within a relatively narrow catalytic pocket.

Gallic acid always showed a particular pose within the active site, favoring the nucleophilic attack by $Thr^1$ to the carbonyl group, with the exception of the GA/$\beta$1 composite model.

All resveratrol/$\beta$ models (with the exception of the $\beta$1i subunit) were characterized by a partial insertion of the polyphenol within the S1 pocket, these singular accommodations (R/$\beta$1i and GA/$\beta$1) yielding to lower affinity complexes.

Ellagic acid showed the highest affinity for the $\beta$5i subunit, being the only complex characterized by a significant hydrophobic interaction with the S1 pocket. Moreover, the EA/$\beta$2i complex reveals a very poor insertion of the ligand into the catalytic site resulting in a lower affinity (Figure 5).

The van der Waals component resulted in the most relevant contribution to the interaction (see Table 1), revealing a moderate hydrophobic feature of the proteasome catalytic sites, and no significant correlation between polyphenol inhibitory efficacy and the hydrophilic direct targeting to

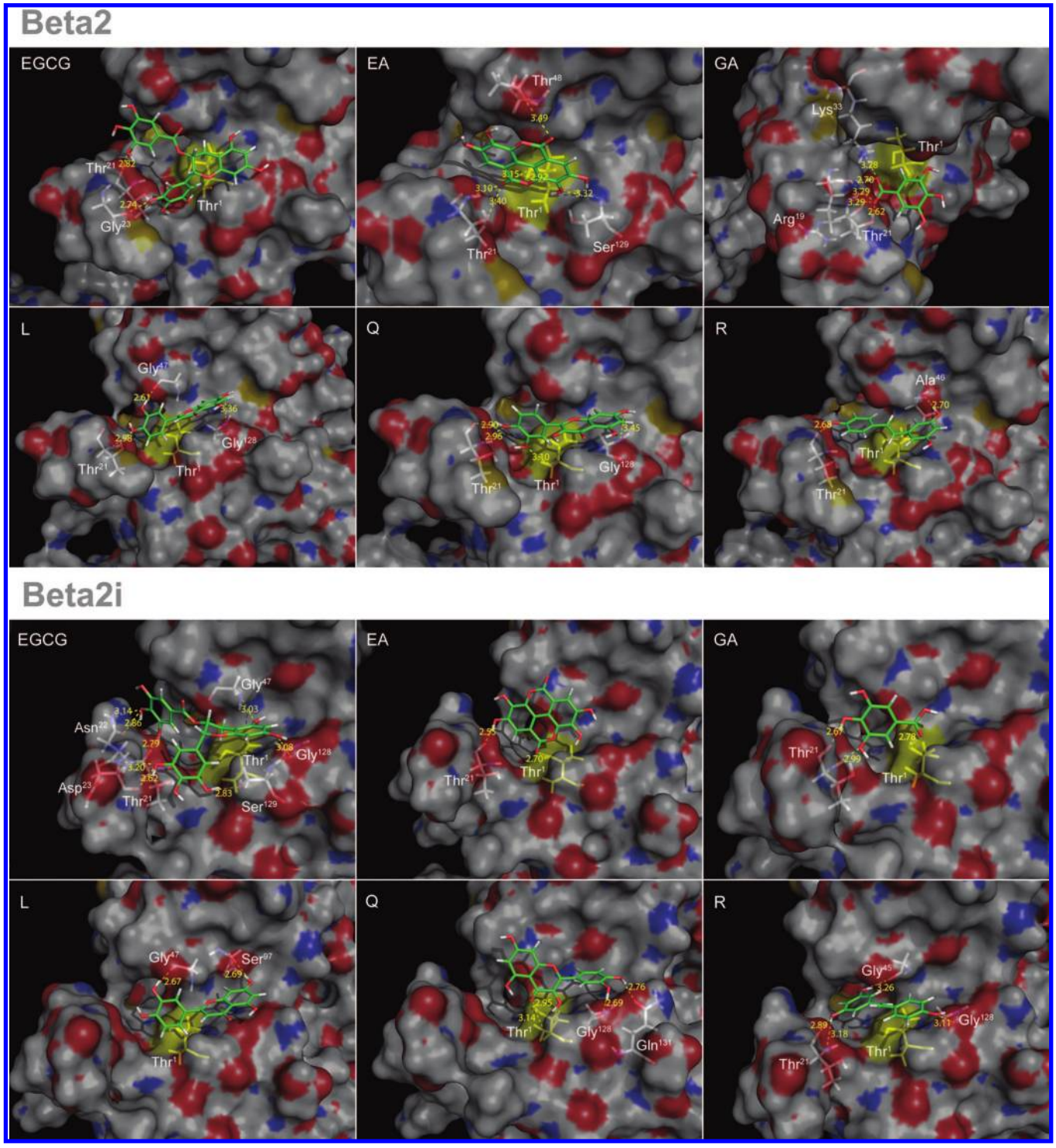


**Figure 5.** Three-dimensional representation of molecular docking of all polyphenols onto $\beta$2 and $\beta$2i subunits (see the Figure 4 legend for details).

catalytic residues (Thr[1], Lys[33], Asp[17])[69] were exploited. However, some complexes, like GA/$\beta$1 and GA/$\beta$1i (Table 1), showed a considerable electrostatic component, due to the number and optimal length of H-bonds formed. In fact, this phenolic ligand possesses a large number of H-bond donor/acceptor atoms (50% of total).

Our results of the *in silico* analysis (Table 1) confirmed the overall behavior reported by the *in vitro* inhibitory studies and summarized in Table 2. In particular, we reported experimental equilibrium constants derived from the enzymatic activities (PGPH, T-Lm, and ChT-L) each one univocally related to a single subunit ($\beta$1, $\beta$2, and $\beta$5, respectively). Moreover, the clioquinol/$\beta$5 complex presents a predicted equilibrium constant of about 100 mM, in agreement with the extremely low inhibition capacity exerted by this molecule on the ChT-L activity.[60] Anyway, the predicted value of the affinity constant is above the range of very weak interactions of macromolecules with their ligands.[70,71]

While the experimental equilibrium constants were measured using the whole 20S complex, the constants obtained by the docking analysis were predicted using the single proteasome subunits. Interestingly, the experimental equi-

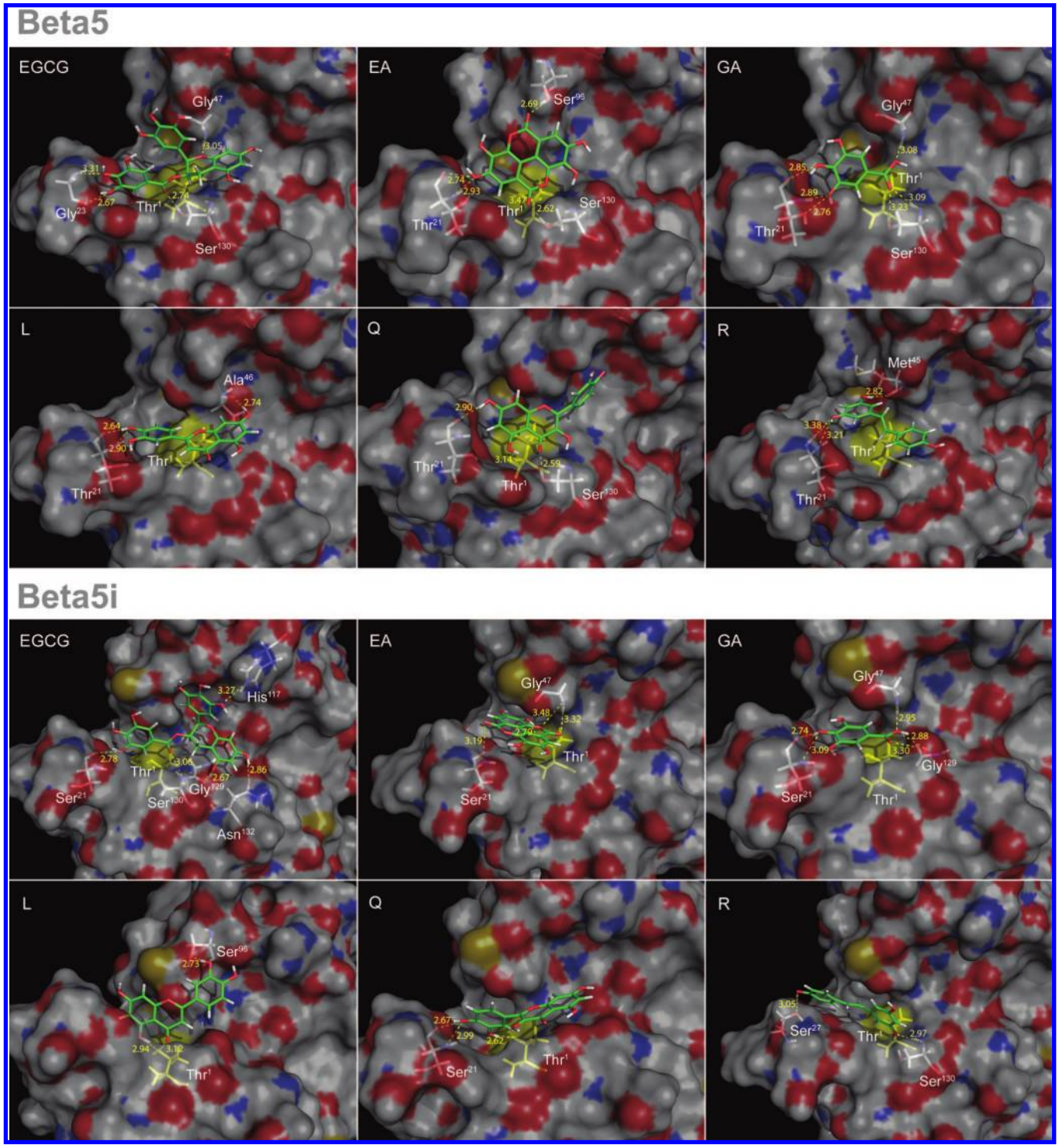


**Figure 6.** Three-dimensional representation of molecular docking of all polyphenols onto $\beta$5 and $\beta$5i subunits (see Figure 4 legend for details).

librium constants and the predicted equilibrium constants were linear dependent (see Figure 3).

In other words, $K_{i,\mathrm{exp}}/K_{i,pred} = Const$ or $\Delta G_{\mathrm{exp}} - \Delta G_{pred} = \Delta\Delta G = Const$. $\Delta G_{\mathrm{exp}}$ could be tentatively attributed to the binding free energy of the single subunit plus the contribution of the quaternary conformational changes or $\Delta G_{\mathrm{exp}} = \Delta G_{tert} + \Delta G_{quater}$. Conversely, $\Delta G_{pred}$ reduces to the binding free energy due to the single subunit $\Delta G_{pred} = \Delta G_{tert}$. So $\Delta\Delta G = \Delta G_{quater}$. The $\Delta\Delta G$ value is common to all the subunits of both constitutive and immunoproteasome, revealing no differential effect on proteasomes' quaternary structure upon the binding of each flavonoids, being instead the differences in binding affinity between a different proteasome subunit and the polyphenols mainly attributable to the peculiarities of each subunit (tertiary structure)—polyphenol biorecognition process.

On the basis of this evidence of polyphenols-mediated proteasome inhibition, we could develop a predictive docking study to rationalize the binding mode of polyphenols to the proteasome and examine the relationship between the differences in their structure and their experimentally measured properties. In particular, in order to formulate a rational

**Table 2.** $K_i$ Values of the Interaction between Polyphenols and Proteasomes Calculated from the $IC_{50}$ Values Reported by Pettinari et al.[48]

| | | $K_i$ (mM) | | |
|---|---|---|---|---|
| | | PGPH | T-L | ChT-L |
| EGCG | *constitutive* | 1.889 ± 0.133 | 0.032 ± 0.007 | 0.063 ± 0.017 |
| | *immuno* | 0.207 ± 0.031 | 0.004 ± 0.001 | 0.006 ± 0.001 |
| EA | *constitutive* | 1.411 ± 0.167 | 0.326 ± 0.021 | 0.663 ± 0.191 |
| | *immuno* | 0.134 ± 0.045 | 3.707 ± 0.370[a] | 0.146 ± 0.013 |
| GA | *constitutive* | 2.722 ± 0.606 | 0.025 ± 0.015 | 0.206 ± 0.029 |
| | *immuno* | 0.578 ± 0.064 | 0.148 ± 0.015 | 0.039 ± 0.005 |
| Q | *constitutive* | 0.088 ± 0.006[a] | 0.158 ± 0.050 | 0.889 ± 0.091 |
| | *immuno* | 0.241 ± 0.061 | 0.154 ± 0.043 | 0.134 ± 0.016 |
| L | *constitutive* | 8.722 ± 6.667 | 1.360 ± 0.335 | 0.820 ± 0.117 |
| | *immuno* | 0.793 ± 0.105 | 0.211 ± 0.108[a] | 0.245 ± 0.014 |
| R | *constitutive* | 0.809 ± 0.475[a] | 1.011 ± 0.165 | 0.460 ± 0.140 |
| | *immuno* | 4.531 ± 0.704 | 0.527 ± 0.084 | 0.104 ± 0.032 |

[a] $K_i$ values were measured according to the procedure described in the Methods section.

design of polyphenols as inhibitors of proteasome activities, our model assumes that polyphenols exert their inhibitory activity specifically targeting proteasome active sites. In detail, the interaction between the S1 pocket and the A-C ring (or another hydrophobic group) partly increases the stability of the polyphenols/proteasome complex, whereas the proximity of a hydrolyzable bond and/or an electrophilic group to the N-terminal $Thr^1$ further stabilizes the polyphenol/proteasome complex, as predicted by previous studies.[65,66] Additionally, polyphenols that are able to insert within the narrow groove of the active site possess a higher inhibitory capacity on the proteasomal activity.

## CONCLUSIONS

The proteasome is one of the most attractive topics in current biological, biochemical, and pharmacological research, and the number of studies focusing on its inhibition/regulation is massive. In this context, small ligands (both natural and synthetic) gained particular attention. Our computational analysis, supported by the validation of experimental evidence, provided a rationalization of the binding mode of natural occurring polyphenols to the 20S mammalian proteasomes. In particular, we observed a fully comparable behavior for the single and assembled subunits upon the binding of a small ligand. Therefore, these original data could be extremely helpful in the screening, design, and development of site-directed 20S proteasome (pro)drugs, starting from a single proteasome subunit, as proposed by other authors,[65,66] rather than from the whole complex.

Conclusively, our results proved the importance of *in silico* strategies for the screening of ligands that can bind to macromolecules with both available and unavailable crystallographic structure and additionally supports the usefulness of computational modeling in the understanding of their molecular mechanisms of action.

**Abbreviations.** EGCG, (-)-epigallocatechin-3-gallate; EA, ellagic acid; GA, gallic acid; Q, quercetin; L, luteolin; R, resveratrol.

## REFERENCES AND NOTES


(1) Fernandez-Recio, J.; Totrov, M.; Skorodumov, C.; Abagyan, R. Optimal docking area: a new method for predicting protein-protein interaction sites. *Proteins* **2005**, *58* (1), 134–143.

(2) Lensink, M. F.; Mendez, R.; Wodak, S. J. Docking and scoring protein complexes: CAPRI 3rd Edition. *Proteins* **2007**, *69* (4), 704–718.

(3) Ruvinsky, A. M.; Vakser, I. A. Interaction cutoff effect on ruggedness of protein-protein energy landscape. *Proteins* **2008**, *70* (4), 1498–1505.

(4) Liu, Z.; Guo, J. T.; Li, T.; Xu, Y. Structure-based prediction of transcription factor binding sites using a protein-DNA docking approach. *Proteins* **2008**, *72* (4), 1114–1124.

(5) Sternberg, M. J.; Gabb, H. A.; Jackson, R. M. Predictive docking of protein-protein and protein-DNA complexes. *Curr. Opin. Struct. Biol.* **1998**, *8* (2), 250–256.

(6) Floquet, N.; Marechal, J. D.; Badet-Denisot, M. A.; Robert, C. H.; Dauchez, M.; Perahia, D. Normal mode analysis as a prerequisite for drug design: application to matrix metalloproteinases inhibitors. *FEBS Lett.* **2006**, *580* (22), 5130–5136.

(7) Mozzicafreddo, M.; Cuccioloni, M.; Bonfili, L.; Eleuteri, A. M.; Fioretti, E.; Angeletti, M. Antiplasmin activity of natural occurring polyphenols. *Biochim. Biophys. Acta* **2008**, *1784* (7−8), 995–1001.

(8) Mozzicafreddo, M.; Cuccioloni, M.; Eleuteri, A. M.; Fioretti, E.; Angeletti, M. Flavonoids inhibit the amidolytic activity of human thrombin. *Biochimie* **2006**, *88* (9), 1297–1306.

(9) Schafferhans, A.; Klebe, G. Docking ligands onto binding site representations derived from proteins built by homology modelling. *J. Mol. Biol.* **2001**, *307* (1), 407–427.

(10) Beavers, M. P.; Myers, M. C.; Shah, P. P.; Purvis, J. E.; Diamond, S. L.; Cooperman, B. S.; Huryn, D. M.; Smith, A. B., III Molecular Docking of Cathepsin L Inhibitors in the Binding Site of Papain. J. Chem. Inf. Model. 2008.

(11) Guilbert, C.; James, T. L. Docking to RNA via root-mean-square-deviation-driven energy minimization with flexible ligands and flexible targets. *J. Chem. Inf. Model.* **2008**, *48* (6), 1257–1268.

(12) Lybrand, T. P. Ligand-protein docking and rational drug design. *Curr. Opin. Struct. Biol.* **1995**, *5* (2), 224–228.

(13) Johnson, M. S.; Srinivasan, N.; Sowdhamini, R.; Blundell, T. L. Knowledge-based protein modeling. *Crit. Rev. Biochem. Mol. Biol.* **1994**, *29* (1), 1–68.

(14) Nayeem, A.; Sitkoff, D.; Krystek, S., Jr. A comparative study of available software for high-accuracy homology modeling: from sequence alignments to structural models. *Protein Sci.* **2006**, *15* (4), 808–824.

(15) Bohm, H. J. Prediction of binding constants of protein ligands: a fast method for the prioritization of hits obtained from de novo design or 3D database search programs. *J. Comput.-Aided Mol. Des.* **1998**, *12* (4), 309–323.

(16) Sova, M.; Perdih, A.; Kotnik, M.; Kristan, K.; Rizner, T. L.; Solmajer, T.; Gobec, S. Flavonoids and cinnamic acid esters as inhibitors of fungal 17beta-hydroxysteroid dehydrogenase: a synthesis, QSAR and modelling study. *Bioorg. Med. Chem.* **2006**, *14* (22), 7404–7418.

(17) Zhou, Z.; Madrid, M.; Madura, J. D. Docking of non-nucleoside inhibitors: neotripterifordin and its derivatives to HIV-1 reverse transcriptase. *Proteins* **2002**, *49* (4), 529–542.

(18) Coux, O.; Tanaka, K.; Goldberg, A. L. Structure and functions of the 20S and 26S proteasomes. *Annu. Rev. Biochem.* **1996**, *65*, 801–847.

(19) Goldberg, A. L. Functions of the proteasome: the lysis at the end of the tunnel. *Science* **1995**, *268* (5210), 522–523.

(20) Groll, M.; Ditzel, L.; Lowe, J.; Stock, D.; Bochtler, M.; Bartunik, H. D.; Huber, R. Structure of 20S proteasome from yeast at 2.4 A resolution. *Nature* **1997**, *386* (6624), 463–471.

(21) Unno, M.; Mizushima, T.; Morimoto, Y.; Tomisugi, Y.; Tanaka, K.; Yasuoka, N.; Tsukihara, T. The structure of the mammalian 20S proteasome at 2.75 A resolution. *Structure* **2002**, *10* (5), 609–618.

(22) Bochtler, M.; Ditzel, L.; Groll, M.; Hartmann, C.; Huber, R. The proteasome. *Annu. Rev. Biophys. Biomol. Struct.* **1999**, *28*, 295–317.

(23) Brannigan, J. A.; Dodson, G.; Duggleby, H. J.; Moody, P. C.; Smith, J. L.; Tomchick, D. R.; Murzin, A. G. A protein catalytic framework with an N-terminal nucleophile is capable of self-activation. *Nature* **1995**, *378* (6555), 416–419.

(24) Seemuller, E.; Lupas, A.; Baumeister, W. Autocatalytic processing of the 20S proteasome. *Nature* **1996**, *382* (6590), 468–471.

(25) Kloetzel, P. M. Antigen processing by the proteasome. *Nat. Rev. Mol. Cell Biol.* **2001**, *2* (3), 179–187.

(26) Niedermann, G.; Geier, E.; Lucchiari-Hartz, M.; Hitziger, N.; Ramsperger, A.; Eichmann, K. The specificity of proteasomes: impact on MHC class I processing and presentation of antigens. *Immunol. Rev.* **1999**, *172*, 29–48.

(27) Rock, K. L.; Goldberg, A. L. Degradation of cell proteins and the generation of MHC class I-presented peptides. *Annu. Rev. Immunol.* **1999**, *17*, 739–779.

(28) Pamer, E.; Cresswell, P. Mechanisms of MHC class I--restricted antigen processing. *Annu. Rev. Immunol.* **1998**, *16*, 323–358.

(29) Paganga, G.; Miller, N.; Rice-Evans, C. A. The polyphenolic content of fruit and vegetables and their antioxidant activities. What does a serving constitute. *Free Radical Res.* **1999**, *30* (2), 153–162.

(30) Akiyama, H.; Sakushima, J.; Taniuchi, S.; Kanda, T.; Yanagida, A.; Kojima, T.; Teshima, R.; Kobayashi, Y.; Goda, Y.; Toyoda, M. Antiallergic effect of apple polyphenols on the allergic model mouse. *Biol. Pharm. Bull.* **2000**, *23* (11), 1370–1373.
(31) Sartor, L.; Pezzato, E.; Dell'Aica, I.; Caniato, R.; Biggin, S.; Garbisa, S. Inhibition of matrix-proteases by polyphenols: chemical insights for anti-inflammatory and anti-invasion drug design. *Biochem. Pharmacol.* **2002**, *64* (2), 229–237.
(32) Tipoe, G. L.; Leung, T. M.; Hung, M. W.; Fung, M. L. Green tea polyphenols as an anti-oxidant and anti-inflammatory agent for cardiovascular protection. *Cardiovasc. Hematol. Disord.: Drug Targets* **2007**, *7* (2), 135–144.
(33) Moridani, M. Y.; Pourahmad, J.; Bui, H.; Siraki, A.; O'Brien, P. J. Dietary flavonoid iron complexes as cytoprotective superoxide radical scavengers. *Free Radical Biol. Med.* **2003**, *34* (2), 243–253.
(34) Miller, A. B. Diet and cancer. A review. *Acta Oncol.* **1990**, *29* (1), 87–95.
(35) Davis, J. N.; Kucuk, O.; Sarkar, F. H. Genistein inhibits NF-kappa B activation in prostate cancer cells. *Nutr. Cancer* **1999**, *35* (2), 167–174.
(36) Hanasaki, Y.; Ogawa, S.; Fukui, S. The correlation between active oxygens scavenging and antioxidative effects of flavonoids. *Free Radical Biol. Med.* **1994**, *16* (6), 845–850.
(37) Nanjo, F.; Goto, K.; Seto, R.; Suzuki, M.; Sakai, M.; Hara, Y. Scavenging effects of tea catechins and their derivatives on 1,1-diphenyl-2-picrylhydrazyl radical. *Free Radical Biol. Med.* **1996**, *21* (6), 895–902.
(38) Yokozawa, T.; Chen, C. P.; Dong, E.; Tanaka, T.; Nonaka, G. I.; Nishioka, I. Study on the inhibitory effect of tannins and flavonoids against the 1,1-diphenyl-2 picrylhydrazyl radical. *Biochem. Pharmacol.* **1998**, *56* (2), 213–222.
(39) Melzig, M. F.; Loser, B.; Ciesielski, S. Inhibition of neutrophil elastase activity by phenolic compounds from plants. *Pharmazie* **2001**, *56* (12), 967–970.
(40) Vitseva, O.; Varghese, S.; Chakrabarti, S.; Folts, J. D.; Freedman, J. E. Grape seed and skin extracts inhibit platelet function and release of reactive oxygen intermediates. *J. Cardiovasc. Pharmacol.* **2005**, *46* (4), 445–451.
(41) Jedinak, A.; Maliar, T.; Grancai, D.; Nagy, M. Inhibition activities of natural products on serine proteases. *Phytother. Res.* **2006**, *20* (3), 214–217.
(42) Kim, M. H. Flavonoids inhibit VEGF/bFGF-induced angiogenesis in vitro by inhibiting the matrix-degrading proteases. *J. Cell Biochem.* **2003**, *89* (3), 529–538.
(43) Spina, M.; Cuccioloni, M.; Mozzicafreddo, M.; Montecchia, F.; Pucciarelli, S.; Eleuteri, A. M.; Fioretti, E.; Angeletti, M. Mechanism of inhibition of wt-dihydrofolate reductase from E. coli by tea epigallocatechin-gallate. *Proteins* **2008**, *72* (1), 240–251.
(44) Navarro-Peran, E.; Cabezas-Herrera, J.; Garcia-Canovas, F.; Durrant, M. C.; Thorneley, R. N.; Rodriguez-Lopez, J. N. The antifolate activity of tea catechins. *Cancer Res.* **2005**, *65* (6), 2059–2064.
(45) Navarro-Peran, E.; Cabezas-Herrera, J.; Hiner, A. N.; Sadunishvili, T.; Garcia-Canovas, F.; Rodriguez-Lopez, J. N. Kinetics of the inhibition of bovine liver dihydrofolate reductase by tea catechins: origin of slow-binding inhibition and pH studies. *Biochemistry* **2005**, *44* (20), 7512–7525.
(46) Dangles, O.; Dufour, C.; Manach, C.; Morand, C.; Remesy, C. Binding of flavonoids to plasma proteins. *Methods Enzymol.* **2001**, *335*, 319–333.
(47) Nam, S.; Smith, D. M.; Dou, Q. P. Ester bond-containing tea polyphenols potently inhibit proteasome activity in vitro and in vivo. *J. Biol. Chem.* **2001**, *276* (16), 13322–13330.
(48) Pettinari, A.; Amici, M.; Cuccioloni, M.; Angeletti, M.; Fioretti, E.; Eleuteri, A. M. Effect of polyphenolic compounds on the proteolytic activities of constitutive and immuno-proteasomes. *Antioxid. Redox Signaling* **2006**, *8* (1−2), 121–129.
(49) Schwede, T.; Kopp, J.; Guex, N.; Peitsch, M. C. SWISS-MODEL: An automated protein homology-modeling server. *Nucleic Acids Res.* **2003**, *31* (13), 3381–3385.
(50) Peitsch, M. C. ProMod: Automated knowledge-based protein modelling tool. *PDB Q. Newslett.* **1995**, *72*, 4.
(51) Van Gunsteren, W. F.; Billeter, S. R.; Eising, A. A.; Hunenberger, P. H.; Kruger, P.; Mark, A. E.; Scott, W. R. P.; Tironi, I. G. *Biomolecular Simulation: The GROMOS96 Manual and User Guide*; Vdf Hochschulverlag AG an der ETH Zurich: Zurich, Switzerland, 1996.
(52) Groll, M.; Bajorek, M.; Kohler, A.; Moroder, L.; Rubin, D. M.; Huber, R.; Glickman, M. H.; Finley, D. A gated channel into the proteasome core particle. *Nat. Struct. Biol.* **2000**, *7* (11), 1062–1067.
(53) Groll, M.; Kim, K. B.; Kairies, N.; Crews, C. Crystal Structure of Epoxomicin:20S Proteasome reveals a molecular basis for selectivity of alpha,beta-Epoxyketone Proteasome Inhibitors. *J. Am. Chem. Soc.* **2000**, *122*, 1237–1238.
(54) Groll, M.; Berkers, C. R.; Ploegh, H. L.; Ovaa, H. Crystal structure of the boronic acid-based proteasome inhibitor bortezomib in complex with the yeast 20S proteasome. *Structure* **2006**, *14* (3), 451–456.
(55) Groll, M.; Huber, R.; Potts, B. C. Crystal structures of Salinosporamide A (NPI-0052) and B (NPI-0047) in complex with the 20S proteasome reveal important consequences of beta-lactone ring opening and a mechanism for irreversible binding. *J. Am. Chem. Soc.* **2006**, *128* (15), 5136–5141.
(56) Groll, M.; Koguchi, Y.; Huber, R.; Kohno, J. Crystal structure of the 20 S proteasome:TMC-95A complex: a non-covalent proteasome inhibitor. *J. Mol. Biol.* **2001**, *311* (3), 543–548.
(57) Forster, A.; Masters, E. I.; Whitby, F. G.; Robinson, H.; Hill, C. P. The 1.9 A structure of a proteasome-11S activator complex and implications for proteasome-PAN/PA700 interactions. *Mol. Cell* **2005**, *18* (5), 589–599.
(58) Berman, H. M.; Westbrook, J.; Feng, Z.; Gilliland, G.; Bhat, T. N.; Weissig, H.; Shindyalov, I. N.; Bourne, P. E. The Protein Data Bank. *Nucleic Acids Res.* **2000**, *28* (1), 235–242.
(59) Laskowski, R. A.; MacArthur, M. W.; Moss, D. S.; Thornton, J. M. PROCHECK: a program to check the stereochemical quality of protein structures. *J. Appl. Crystallogr.* **1993**, *26*, 283–291.
(60) Daniel, K. G.; Chen, D.; Orlu, S.; Cui, Q. C.; Miller, F. R.; Dou, Q. P. Clioquinol and pyrrolidine dithiocarbamate complex with copper to form proteasome inhibitors and apoptosis inducers in human breast cancer cells. *Breast Cancer Res.* **2005**, *7* (6), R897−908.
(61) Chew, L. P.; Huttenlocher, D.; Kedem, K.; Kleinberg, J. Fast detection of common geometric substructure in proteins. *J. Comput. Biol.* **1999**, *6* (3−4), 313–325.
(62) Eleuteri, A. M.; Angeletti, M.; Lupidi, G.; Tacconi, R.; Bini, L.; Fioretti, E. Isolation and characterization of bovine thymus multicatalytic proteinase complex. *Protein Expression Purif.* **2000**, *18* (2), 160–168.
(63) Orlowski, M.; Cardozo, C.; Michaud, C. Evidence for the presence of five distinct proteolytic components in the pituitary multicatalytic proteinase complex. Properties of two components cleaving bonds on the carboxyl side of branched chain and small neutral amino acids. *Biochemistry* **1993**, *32* (6), 1563–1572.
(64) Amici, M.; Lupidi, G.; Angeletti, M.; Fioretti, E.; Eleuteri, A. M. Peroxynitrite-induced oxidation and its effects on isolated proteasomal systems. *Free Radical Biol. Med.* **2003**, *34* (8), 987–996.
(65) Chen, D.; Daniel, K. G.; Chen, M. S.; Kuhn, D. J.; Landis-Piwowar, K. R.; Dou, Q. P. Dietary flavonoids as proteasome inhibitors and apoptosis inducers in human leukemia cells. *Biochem. Pharmacol.* **2005**, *69* (10), 1421–1432.
(66) Smith, D. M.; Daniel, K. G.; Wang, Z.; Guida, W. C.; Chan, T. H.; Dou, Q. P. Docking studies and model development of tea polyphenol proteasome inhibitors: applications to rational drug design. *Proteins* **2004**, *54* (1), 58–70.
(67) Kleywegt, G. J.; Jones, T. A. Phi/psi-chology: Ramachandran revisited. *Structure* **1996**, *4* (12), 1395–1400.
(68) Kuhn, D. J.; Burns, A. C.; Kazi, A.; Dou, Q. P. Direct inhibition of the ubiquitin-proteasome pathway by ester bond-containing green tea polyphenols is associated with increased expression of sterol regulatory element-binding protein 2 and LDL receptor. *Biochim. Biophys. Acta* **2004**, *1682* (1−3), 1–10.
(69) Groll, M.; Huber, R. Inhibitors of the eukaryotic 20S proteasome core particle: a structural approach. *Biochim. Biophys. Acta* **2004**, *1695* (1−3), 33–44.
(70) Amiconi, G.; Bertollini, A.; Bellelli, A.; Coletta, M.; Condo, S. G.; Brunori, M. Evidence for two oxygen-linked binding sites for polyanions in dromedary hemoglobin. *Eur. J. Biochem.* **1985**, *150* (2), 387–393.
(71) Shimura, K.; Kasai, K. Determination of the affinity constants of concanavalin A for monosaccharides by fluorescence affinity probe capillary electrophoresis. *Anal. Biochem.* **1995**, *227* (1), 186–194.

CI800235M